

# Fast fluorescence lifetime imaging of calcium in living cells

## A. V. Agronskaia

Utrecht University  
Debye Institute  
Department of Molecular Biophysics  
P.O. Box 80000  
3508 TA Utrecht, The Netherlands

## L. Tertoolen

KNAW Hubrecht Laboratory  
Netherlands Institute for Developmental Biology (NIOB)  
Uppsalalaan 8  
3584 CT Utrecht, The Netherlands

## H. C. Gerritsen

Utrecht University  
Debye Institute  
Department of Molecular Biophysics  
P.O. Box 80000  
3508 TA Utrecht, The Netherlands  
E-mail: h.c.gerritsen@phys.uu.nl

**Abstract.** A fast fluorescence lifetime imaging (FLIM) system is developed that can acquire images at a rate of hundreds of frames per second. The FLIM system is based on a wide-field microscope equipped with a time-gated intensified CCD detector and a pulsed laser. The time-gated detector acquires the signals from two time gates simultaneously and is therefore insensitive to movements of the specimen and photo-bleaching. The system is well suited for quantitative biological FLIM experiments and its performance is evaluated in calcium imaging experiments on beating neonatal rat myocytes. Several calcium sensitive dyes are characterized and tested for their suitability for fast FLIM experiments: Oregon Green Bapta-1 (OGB1), Oregon Green Bapta-2 (OGB2), and Oregon Green Bapta-5N (OGB5N). Overall the sensitivity range of these dyes is shifted to low calcium concentrations when used as lifetime dyes. OGB1 and OGB2 behave very similarly and can be used for FLIM-based calcium imaging in the range 1 to ~500 nM and OGB5N can be used up to 3  $\mu$ M. The fast FLIM experiments on the myocytes could be carried out at a 100-Hz frame rate. During the beating of the myocytes a lifetime change of about 20% is observed. From the lifetime images a rest calcium level of about 65 nM is found. © 2004 Society of Photo-Optical Instrumentation Engineers. [DOI: 10.1117/1.1806472]

Keywords: fast fluorescence lifetime imaging; calcium imaging; Oregon Green Bapta dyes; neonatal rat myocytes.

Paper 03129 received Oct. 29, 2003; revised manuscript received Mar. 26, 2004; accepted for publication May 19, 2004.

## 1 Introduction

Changes in free calcium concentration play an important role in many biological processes including muscle contraction, neuronal activity, and the regulation of metabolism. Therefore, much effort has been spent on the development of systems for imaging calcium fluxes. The two main challenges in this area are: (1) the imaging of intracellular calcium at frame rates exceeding video rate, and (2) the quantification of intracellular calcium. Although in recent years, the detection speed in fluorescence microscopy reached the millisecond range,<sup>1,2</sup> the interpretation and quantification of the fluorescence intensity measurements is not straightforward and can be hampered by, for instance, nonhomogeneous staining of cells and photobleaching of the fluorescent dye.

Ratiometric imaging methods<sup>3–5</sup> can be employed to quantify calcium or other ions. Here, fluorescent probes are employed that exhibit distinct shifts in their spectral properties upon binding to calcium ions. In general, two fluorescence images are acquired, either at different excitation wavelength using the same detection wavelength band, or at one excitation wavelength using two different detection wavelength bands. When probes exhibit shifts in the excitation or emission spectra upon changes in the biological conditions, the ratio of the two fluorescence images can be used to recon-

struct the intracellular conditions. However, the calibration of the response of the ratiometric probes is not straightforward and usually needs to be carried out on the specimen under investigation. Calibration curves obtained from buffer solutions may differ significantly from calibration curves recorded in cells. In the case of calcium imaging, most of the ratiometric calcium probes require UV excitation, which is potentially harmful for cells and may cause high levels of autofluorescence.

Visible light excited calcium probes usually show no calcium dependent changes in their excitation or emission spectra. In general, only changes of their quantum yield and, therefore, of their fluorescence intensity occur. A few methods have been developed to extract quantitative data from measurements with these dyes.<sup>6</sup> The disadvantage of all these methods is that a calibration procedure needs to be carried out on each specimen.

The fluorescence lifetime of fluorescent ion indicators can also be employed for imaging. In general the fluorescence lifetime is independent of factors that influence the fluorescence intensity such as dye concentration and fading due to photobleaching. Fluorescence lifetime imaging (FLIM) can be employed for quantitative calcium imaging.<sup>7,8</sup> Here, the (average) lifetime is a direct measure of the ion concentration. For several dyes it was demonstrated<sup>9,10</sup> that fluorescence lifetime based ion sensing does not require a calibration in cells;

Address all correspondence to Hans Gerritsen, Utrecht Univ., Debye Institute, Molecular Biophysics Section, P.O. Box 80000, NL-3508 Utrecht, Netherlands. E-mail: H.C.Gerritsen@phys.uu.nl

a calibration carried out on a series of buffers suffices.

So far, a drawback of fluorescence lifetime imaging for biological studies is the comparatively slow acquisition rate: typical acquisition times required for fluorescence lifetime images are on the order of many seconds. Two exceptions can be found in recent literature showing frequency-domain-based FLIM at video rate (25 frames per sec).<sup>11,12</sup>

We previously implemented time-gating-based FLIM in confocal<sup>13</sup> and multiphoton excitation<sup>14</sup> microscopes. Despite the fact that these are scanning microscopes, lifetime images could be recorded in as little as 1 sec. In wide-field microscopy all pixels are acquired in parallel and therefore this method is intrinsically much faster than point-scanning microscopy. In the wide-field fast FLIM microscope used here, two time gates are employed. Both time gates are detected simultaneously after every excitation pulse by the same detector. This makes the microscope insensitive to intensity variations introduced by instabilities of the light source, fading due to photo bleaching, and movements of the specimen.

We investigated the feasibility of fast imaging of calcium fluxes by means of fluorescence lifetime imaging. This work includes the characterization of the fluorescence lifetime behavior of several Oregon Green Bapta based dyes. The viability of the fast FLIM method is illustrated by the imaging of calcium fluxes in beating neonatal rat myocytes at a frame rate of 100 Hz.

## 2 Material and Methods

### 2.1 Fast FLIM Setup

The fast FLIM setup employed here is based on a wide-field epi-fluorescence microscope. It is equipped with a two-channel time-gated detector and employs a pulsed excitation source. The fluorescence lifetime is obtained from the ratio of the two gate intensities  $I_A$  and  $I_B$  with the formula:

$$\tau_{fl} = \frac{\Delta t}{\ln(I_A/I_B)}, \quad (1)$$

where  $\Delta t$  is the time offset between the two gates. In the case of a monoexponential decay this equation provides an exact fluorescence lifetime. In the case of multiexponential decay, Eq. (1) yields an "average" fluorescence lifetime ( $\tau_{aver}$ ). The exact value of this lifetime depends on the precise details of the gate settings (time offset of first gate, width of gates, and delay between gates). Multiexponential decays can be recorded by increasing the number of gates.<sup>15,16</sup>

In the wide-field FLIM setup a single time-gated intensified CCD camera detects both fluorescence intensities  $I_A$  and  $I_B$  simultaneously. This is achieved by splitting the fluorescence image into two images, optically delaying one of the images, and finally focusing both images on different sections of the detector. A detailed description of the time-gated detector can be found elsewhere.<sup>17</sup> The setup (see Fig. 1) consists of a commercial titanium-sapphire laser with pulse width <2 ps (Tsunami, Spectra-Physics Inc., Mountain View, CA, USA). The fundamental output of the laser is frequency doubled by a LBO crystal (EKSMa, Vilnius, Lithuania) and the repetition rate is decreased to 8.2 MHz by a fast acousto-optical modulator (MT-08, A.A.sa, St-Rémy-Lès-Chevreuse, France). The excitation laser light is coupled into an inverted

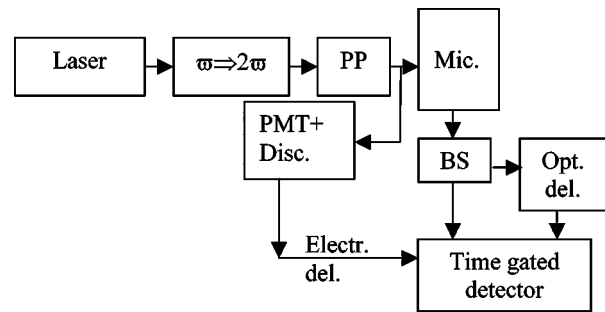


**Fig. 1** Schematic diagram of the fast FLIM microscope: PP—pulse picker; Mic.—microscope; PMT+Disc.—PMT and discriminator; Electr. del.—Electronic delay; BS—beam splitter; Opt. del.—optical delay line.

microscope (Diaphot 300, Nikon, Japan) via an optical fiber (multimode, 0.2 mm, NA=0.16). The collected fluorescence emission is spectrally filtered by a dichroic mirror (DM505, Nikon, Japan) and a long-pass filter (OG515, Schott, Mainz, Germany) and split into two beams by a beam splitter with 87% transmission. This splitting ratio is chosen in order to optimize the use of the 8-bit dynamic range of the CCD camera. At this beam splitter ratio a 2.7-ns fluorescence lifetime yields equal signals for  $I_A$  and  $I_B$ . The reflected beam is optically delayed by 5.05 ns by a relay lens system. The length of the delay line is fixed. Delayed and nondelayed beams are separately focused onto the photocathode of the time-gated image intensifier (V3063U-01W/NESA, Hamamatsu Photonics K.K., Hamamatsu City, Japan), which is fiber coupled to a Generation 1 intensifier (XX1490AD, Delft Electronics Products, Delft, The Netherlands). The output of the last image intensifier is imaged onto a fast, frame-transfer CCD camera (CA-D1\_A, Dalsa Inc., Waterloo, Canada). The chip size of the 8-bit CCD camera is 128×126 pixels, the pixel size is 16×16  $\mu\text{m}$ , and the maximum frame rate amounts to 840 frames per sec.

The trigger signal for the gated image intensifier is obtained from a photo multiplier tube (PMT) (R4832, Hamamatsu Photonics K.K., Hamamatsu City, Japan) that detects a small fraction of the excitation light. The output of this PMT is discriminated by a Philips Scientific discriminator (Model 6915, Ramsey, NJ, USA) and electronically delayed by a homemade delay unit. The length of the electronic delay can be optimized for different applications. The width of the time gate is 5 ns. By triggering the time-gated image intensifier at the right moment, two gated images are recorded simultaneously that contain the time-integrated signals from 0 to 5 ns ( $I_A$ ) and from 5 to 10 ns ( $I_B$ ).

All experiments are carried out with a 40×/1.3 oil immersion microscope objective (Fluor, Nikon, Japan). The excitation wavelength employed in the imaging experiments is 460 nm and the maximum laser power at the specimen is on the order of 0.5 mW (about 60 nW/pixel).

Image acquisition is controlled by homemade software written in the C++ computer language. The images are analyzed using homemade software written in the Interactive Data Language (IDL, Research Systems Inc., Boulder, CO, USA). The main function of the program is to calculate fluorescence lifetime images from the two time-gated images.

First, the CCD images are corrected for the background by a pixel-by-pixel subtraction of a background image. The background image is acquired using a specimen containing only water. After the background correction, the images corresponding to the two time windows are separated and aligned with respect to each other. The alignment is based on the following match procedure. Reference images are recorded of 2- $\mu\text{m}$  fluorescent beads. The two bead images corresponding to the first and second time gate, respectively, are shifted with respect to each other to maximize their overlap. To this end the images are multiplied with each other and the position with the highest correlation is taken to be the optimum position. Other images are aligned with the offsets in the  $x$  and  $y$  directions obtained from this optimum position. Before the ratio is calculated a threshold is applied to the image corresponding to the second time window. The threshold amounts to about one tenth of the maximum value in the image. The fluorescence lifetime image is calculated by dividing the first time window image by the thresholded second time window image. Next, Eq. (1) is used to convert the ratios into average fluorescence lifetimes. Alternatively, the relation between the ratio and average fluorescence lifetime can be obtained from a table containing the ratios for different lifetimes. The latter approach is used in the case of nonequal gate widths that are realized by letting the laser pulse fall within the first gate. Fluorescence intensity images are produced by addition of the first and the second time-window images in correct proportions (13% of the first time window and 87% of the second time window).

The dimensions of the fluorescence lifetime and intensity images are about  $60 \times 120$  pixels. These dimensions are limited by the size of the comparatively small CCD chip.

## 2.2 Spectral and Fluorescence Lifetime Measurements

Absorption spectra of reference solutions of the dyes at different ion concentrations are measured with a standard spectrophotometer (DW2000, SLM-Aminco, Urbana, IL, USA). Emission spectra are acquired using a Perkin Elmer (Shelton, Connecticut, USA) LS 50 B spectrometer at an excitation wavelength of 496 nm. The fluorescence lifetimes of the reference specimens are measured using time-correlated single-photon counting (TCSPC). The details of the TCSPC setup can be found elsewhere.<sup>18</sup>

## 2.3 Sample Preparation

The potassium salts and acetoxymethyl (AM) esters of the calcium sensitive dyes Oregon Green 488 Bapta-1, Bapta-2, and Bapta-5N, as well as the calcium calibration buffer kit are obtained from Molecular Probes (Eugene, OR, USA). Stock solutions of the potassium salts of the dyes (2 mM) are prepared in zero calcium buffers. Directly after preparation, the stock solutions are diluted in 11 different buffers (free  $\text{Ca}^{2+}$  concentration range 0 to 39.8 mM) to a final dye concentration of 2  $\mu\text{M}$ . Solutions of calcium dyes in buffers are stored at 4 °C.

The stock solution of Oregon Green 488 Bapta-1-AM is prepared in DMSO (5 mM), immediately diluted to the final concentration of 10  $\mu\text{M}$  in Tris-buffer, and directly used. The composition of the buffer is NaCl (133 mM), KCl (5 mM),

$\text{CaCl}_2$  (1 mM), Tris (10 mM),  $\text{MgCl}_2 \cdot 6\text{H}_2\text{O}$  (1 mM), and glucose (1 gram/liter); the pH amounts to 7.2.

Neonatal rat myocytes are isolated from 3- to 4-day-old rats. Experiments are carried out on the third day after isolation. After extraction from the growth medium, the cells are carefully washed three times in Tris-buffer and incubated in a 10- $\mu\text{M}$  solution of Oregon Green Bapta-1-AM for 30 min at 37 °C. After incubation the cells are washed three times to remove excess dye. Measurements are performed in the same Tris-buffer at 37 °C.

## 3 Results and Discussion

### 3.1 Optical Properties of Oregon Green Based Calcium Probes

Fluorescent ion indicators usually exist in two states, the ion-bound state and the free state. In general these two states exhibit different photophysical properties. Many of the calcium indicators exhibit different fluorescence lifetimes for the free and ion-bound state<sup>8</sup> and the average lifetime can be directly related to the calcium concentration. Therefore, FLIM can be used for the quantitative imaging of free calcium in (living) cells. Importantly, most calcium indicators that have their absorption bands in the visible part of spectrum can be employed for fluorescence lifetime based quantitative calcium sensing. Thus, using FLIM quantitative calcium imaging is possible without the need for UV excitation.

Here, we investigate the potential of Oregon Green based calcium indicators for fast FLIM of calcium. The optical properties of Oregon Green Bapta-1 (OGB1), Oregon Green Bapta-2 (OGB2), and Oregon Green Bapta-5N (OGB5N) are characterized. These dyes have their absorption maximum at about 496 nm, and their dissociation constants are 170, 580, and 20,000 nM, respectively.

The absorption and the fluorescence spectra of all three dyes are measured in 11 different calcium buffers in the free calcium concentrations range from 0 to 39.8  $\mu\text{M}$ . The absorption spectra of the dyes are not sensitive to the free calcium concentration and the extinction coefficients at 496 nm are found to be 70,000, 118,000, and 53,000  $\text{M}^{-1}\text{cm}^{-1}$  for OGB1, OGB2, and OGB5N, respectively. As expected, there are no calcium concentration dependent changes in the shape of the emission spectra of the dyes. The intensity of the emission increases with increasing free calcium concentration (see Table 1). It is important to note that up to calcium concentrations of 0.6  $\mu\text{M}$ , OGB1 yields the highest fluorescence signal of all three dyes. The dissociation constants of the dye-calcium complexes calculated from the emission intensities are 150 nM, 560 nM, and 20  $\mu\text{M}$  for OGB1, OGB2, and OGB5N, respectively. These values are in good agreement with the values provided by Molecular Probes, i.e., 170 nM, 580 nM, and 20  $\mu\text{M}$ .

In Fig. 2 the fluorescence intensity decays of the dyes are shown. The decay curves are recorded using TCSPC. A biexponential decay is required to describe the results (see Table 2). Fitting to a triexponential decay does not significantly improve the quality of the fits as judged by the  $\chi^2$ . Overall, the quality of the fits is good ( $\chi^2=1.7$  to 3.8). At the lowest calcium concentrations the contribution of the long decay component is very small and consequently the decay curves are more difficult to fit. This results in systematic errors in the

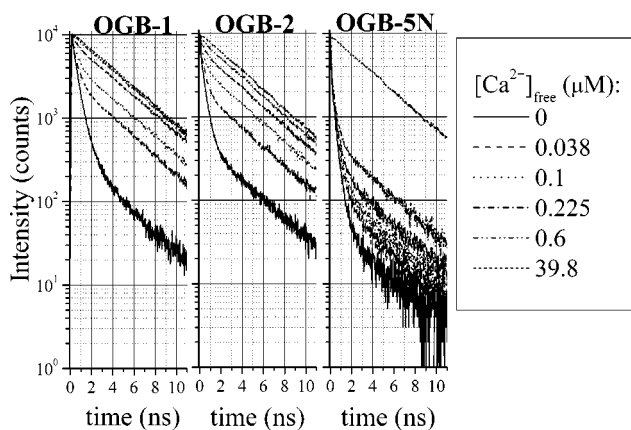
**Table 1** Fluorescence intensity, integrated from 500 to 600 nm, of Oregon Green Bapta-1, Oregon Green Bapta-2, and Oregon Green Bapta-5N in calcium buffers.

[Ca] <sup>2+</sup> <sub>free</sub> (μM)	Average fluorescence intensity (arbitrary units)		
	OGB1	OGB2	OGB5N
0	18	11	5
0.017	32	22	5
0.038	47	28	6
0.065	68	45	6
0.1	81	60	6
0.15	106	88	7
0.225	130	113	7
0.351	162	129	10
0.602	189	158	11
1.35	214	244	19
38.9	218	320	175

fitted lifetimes and amplitudes. When the calcium concentration goes down, the relative amplitudes of the short and long lifetime components go up and down, respectively.

The behavior of OGB2 is very similar to that of OGB1. A systematic error is observed at low calcium concentrations but the fluorescence decays of these two dyes can be fitted with the same set of fluorescence lifetimes of 0.33 ns and 3.7 ns without a significant decrease of the quality of the fit ( $\chi^2 = 1.8$  to 3.9). The lifetime values are in a reasonable agreement with the values of 0.7 and 4.0 ns that are reported for OGB1 by Lakowicz.<sup>8</sup>

The analysis of the fluorescence decay behavior of OGB5N is consistent with that of OGB1 and OGB2. This dye is developed for the detection of free calcium concentrations

**Fig. 2** Fluorescence decays of Oregon Green Bapta-1, Oregon Green Bapta-2, and Oregon Green Bapta-5N measured by TCSPC in different calcium buffers.**Table 2** Fluorescence lifetimes ( $\tau_1, \tau_2$ ) and the amplitudes of the short fluorescence lifetime ( $A_1$ ) as a function of free calcium concentration of Oregon Green Bapta-1, Oregon Green Bapta-2, and Oregon Green Bapta-5N.

[Ca <sup>2+</sup> ] <sub>free</sub> (μM)	OGB1			OGB2			OGB5N		
	$\tau_1$ (ns)	$\tau_2^*$ (ns)	$A_1$ (%)	$\tau_1$ (ns)	$\tau_2^*$ (ns)	$A_1$ (%)	$\tau_1$ (ns)	$\tau_2^*$ (ns)	$A_1$ (%)
0	0.42	2.5	94	0.36	3.5	93	0.25	1.9	97
0.017	0.41	3.6	83	0.33	3.6	85	0.24	2.2	97
0.038	0.38	3.6	70	0.33	3.6	75	0.25	2.4	97
0.065	0.36	3.7	63	0.30	3.6	65	0.27	2.6	96
0.1	0.35	3.7	58	0.29	3.6	58	0.25	2.9	96
0.15	0.33	3.7	43	0.32	3.6	42	0.26	3.0	95
0.225	0.31	3.7	31	0.29	3.6	34	0.24	3.2	95
0.351	0.27	3.7	25	0.28	3.6	27	0.25	3.26	93
0.602	0.29	3.8	8	0.29	3.6	15	0.25	3.4	90
1.35	...	3.7	0	...	3.6	0	0.19	3.6	82
38.9	...	3.7	0	...	3.7	0	...	3.7	0

\*amplitude of the long component ( $A_2$ ) of the fluorescence lifetime  $\tau_2$  is equal to  $(100 - A_1)$  (%)

in the range from 1 to 100 μM. Most of the fluorescence intensity and lifetime measurements on this dye presented here are carried out at comparatively low calcium concentrations. Consequently only small effects of calcium are observed (see Table 1 and Fig. 2).

All the fluorescence decays of OGB5N reveal a short decay component of about 0.25 ns that appears to be insensitive to the free calcium concentration. The long decay component, however, has small amplitude and the fitting procedure yields values that apparently increase with increasing free calcium concentration (see Table 2). This again seems to be due to the systematic errors discussed above. In order to improve the accuracy of the fitting procedure a global fit is carried out of all 11 decay curves with the same two fluorescence decay components. The global fit yields very acceptable fits with lifetimes of 0.25 and 3.65 ns. The quality of the fits as judged by the  $\chi^2$  increases by less than 20% for the individual decay curves.

The above findings indicate that the bound and free OGB dye molecules have distinct fluorescence lifetimes. The relative amplitude of the free fluorescence lifetime component ( $A_1$ ) is a direct measure of the fraction of free dye molecules in solution and the fraction of calcium bound dye molecules amounts to  $1 - A_1(A_2)$ .

In Fig. 3 the  $A_1$  of OGB1, OGB2, and OGB5N as a function of the free calcium concentration is depicted. The figure does not show significant differences between the behavior of OGB1 and OGB2. The amplitudes of  $A_1$  and  $A_2$  of both dyes are reduced to 50% of their maximum value at about 160 nM. The similarity in the lifetime behavior of OGB1 and OGB2

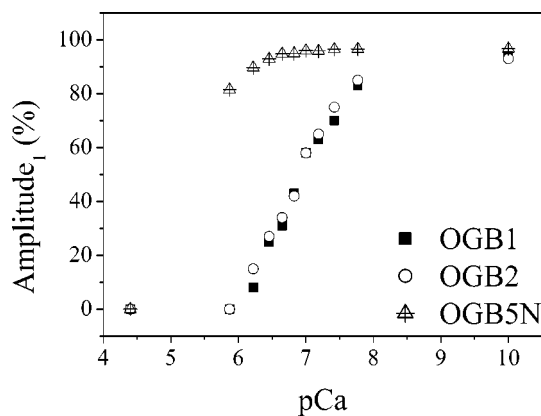


**Fig. 3** Amplitude of short fluorescence lifetime component of OGB1 (0.33 ns), OGB2 (0.33 ns), and OGB5N (0.25 ns) as a function of free calcium concentration. Note the similarity between OGB1 and OGB2.

suggests that the difference in the  $k_D$  of these dyes is only due to the difference in the quantum yield of the free and bound forms of the dyes.<sup>19</sup> For OGB5N the amplitudes are reduced to 50% of their original value at a calcium concentration of 7.5  $\mu$ M.

### 3.2 Calibration of the FLIM Setup

In the fast FLIM setup the fluorescence lifetime is determined from the ratio  $R$  of the fluorescence intensities accumulated in the two time windows. The windows have equal widths of 5 ns (FWHM) and the start of the windows is separated by 5.05 ns. The setup can be optimized for different applications by choosing different offsets in time between the opening of the first gate and the laser pulse. If the first gate is opened before the arrival of the laser pulse, the width of the first time window is effectively decreased.

The response of the time-gated detector is obtained by measuring reflected laser light at a number of different time offsets between the laser pulse and the opening of the first time window.<sup>17</sup> The response to the Oregon Green dyes is calculated by convoluting the fluorescence decays obtained by TCSPC with the detector time response. Next, the fluorescence intensities accumulated in the first and second time window are calculated for different time offsets between the excitation pulse and the start of the first gate, taking into account the beam splitting ratio of 6.5.

The results of these calculations show that the highest integrated fluorescence intensity, the highest value of  $R$ , and the highest sensitivity of  $R$  to the free calcium concentrations are all obtained at different time offsets. The highest fluorescence intensities for all OGB dyes are obtained when the image intensifier is opened about 1 ns before the arrival of the laser pulse (delay time is  $-1$  ns). Here, the delay time is defined as the time with respect to the moment that the gate opens, i.e., when the gain of the intensifier reaches 50% of its final value. The highest values of  $R$  are found when the image intensifier opens at the moment of the arrival of the laser pulse (delay time is 0 ns). The highest dynamic range of  $R$  is obtained when the image intensifier is opened 1.5 ns before the arrival of the laser pulse (delay time is  $-1.5$  ns). The sensitivity

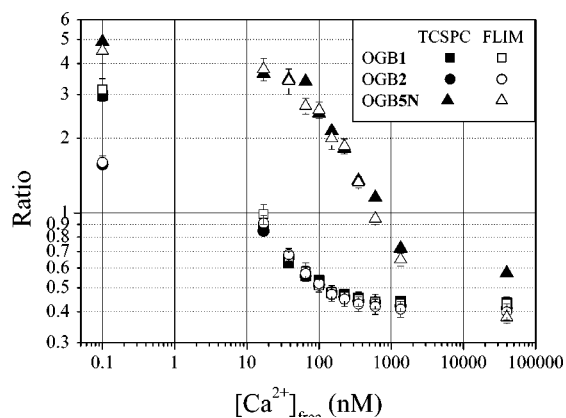


**Fig. 4** Measured gate intensity ratios of Oregon Green Bapta-1 (squares), Bapta-2 (circles), and Bapta-5N (triangles) as a function of free calcium concentration. The closed symbols represent the ratios as calculated from measured fluorescence decays (TCSPC), the open symbols represent the ratios measured with the fast FLIM.

range, however, hardly changes with the shift of the delay time.

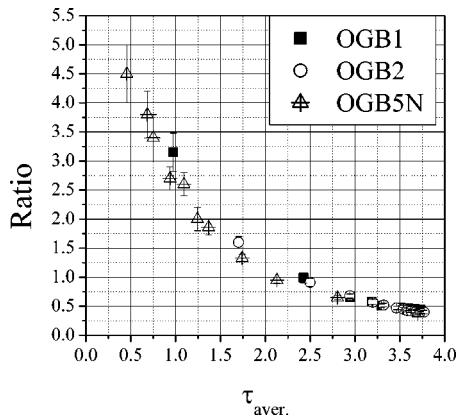
In the calcium imaging experiments described here, a time offset of  $-1.0$  ns is chosen between the laser pulse and the opening of the image intensifier. At this setting the first time window ranges from 0 to 4 ns and the second time window ranges from 4 to 9 ns.

Figure 4 shows measured and calculated values of  $R$  for OGB1, OGB2, and OGB5N in different calcium buffers. The calculated ratios are obtained by convoluting the detector response with the TCSPC measured fluorescence decay curves using a time offset of  $-1$  ns. The calculated and measured data agree very well. Compared with the  $k_D$  values of the dyes, the calcium sensitivity range of the ratio (lifetime) measurements is shifted to lower free calcium values. The 50% points of the ratios are now at 5, 13, and 100 nM of free calcium for OGB1, OGB2, and OGB5N, respectively.

The  $-1.0$ -ns time offset between the laser pulse and the opening of the image intensifier results in nonequal gate widths, therefore the analytical expression in Eq. (1) for the determination of the (average) fluorescence lifetime cannot be used. Here, the average lifetimes are calculated for all OGB dyes in all calcium buffers using Table 2 and

$$\tau_{aver} = \frac{A_1 \cdot \tau_1^2 + A_2 \cdot \tau_2^2}{A_1 \tau_1 + A_2 \tau_2}, \quad (2)$$

where  $A_{1,2}$  and  $\tau_{1,2}$  are the amplitudes and lifetimes of the individual components. The relation between the measured gate intensity ratios ( $R$ ) and the average fluorescence lifetimes of all OGB dyes is shown in Fig. 5. Interestingly, all three dyes show a similar relation between the ratio  $R$  and the average fluorescence lifetime. This is explained by the fact that in all these cases we are dealing with the same family of dyes. Oregon Green Bapta-1 and Oregon Green Bapta-5N only differ in their calcium sensitive (Bapta) part. Oregon Green Bapta-2, however, contains two Oregon Green fluorophores and the interactions of the two fluorophores could influence the fluorescence lifetime and therefore the ratio  $R$ . Nevertheless, OGB2 shows exactly the same relation between the ratio



**Fig. 5** The relation between the gate intensity ratio and the average fluorescence lifetimes for Oregon Green Bapta-1 (■), Oregon Green Bapta-2 (○), and Oregon Green Bapta-5N (△) in different calcium buffers.

$R$  and the average fluorescence lifetime as OGB1 and OGB5N. Therefore, we conclude that little or no interaction occurs between the two fluorescent groups in OGB2.

The Oregon Green Bapta dyes can be employed for quantitative, fluorescence lifetime based calcium sensing. The usable calcium range of the dyes when used in fluorescence lifetime mode is shifted to low free calcium concentrations compared to when used in fluorescence intensity mode. This shift in sensitivity range is caused by the fact that the short lifetime component of the fluorescence decay has a low quantum yield. Consequently, the average fluorescence lifetime and also the ratio  $R$  is dominated by the long lifetime, high quantum-efficiency component, at comparatively low Ca concentrations. Such shifts in sensitivity range are common in FLIM-based calcium sensing.<sup>19</sup>

The dye with the largest lifetime response in the range of 0.1 to 1  $\mu\text{M}$  of  $[\text{Ca}^{2+}]_{\text{free}}$  is OGB5N (see Fig. 4). However, the fluorescence intensity of this dye is about 10 times lower than that of the other OGB dyes (see Table 1). Therefore, OGB5N is not very well suited for fluorescence lifetime based calcium imaging at high frame rates. We notice no significant differences between the lifetime behavior of OGB1 and OGB2. Both dyes can be employed for the quantification of free calcium in the range from 1 to  $\sim 500$  nM. OGB1 yields a stronger fluorescence signal than OGB2 in the fluorescence lifetime sensitivity range of the dyes. Therefore, we have used OGB1 for the fast FLIM measurements presented here. This limits the detectable calcium concentration range in the imaging experiments to concentrations below  $\sim 500$  nM.

### 3.3 Calcium Imaging

The suitability of the fast FLIM setup for the imaging of fast calcium fluxes is evaluated. To this end neonatal rat myocytes stained with Oregon Green 488 Bapta-1-AM are employed. This is a convenient test system since the neonatal myocytes contract spontaneously at a frequency of about 0.5 to 1.5 Hz (at 37 °C). The contraction is accompanied by an increase of the free  $\text{Ca}^{+2}$  concentration in the cells from  $\sim 100$  nM in rest to  $> 1.5$   $\mu\text{M}$  in the peak.<sup>20–23</sup> The concentration rise time is in the order of 10 to 100 ms. The response time of Oregon Green Bapta 1 is approximately 5 ms,<sup>24</sup> therefore, this dye is a useful

indicator for following such fast changes in free calcium concentration. The drawback of employing the neonatal myocytes is that the peak calcium concentration amounts to about 1.5  $\mu\text{M}$ , well above the maximum of the sensitivity range of OGB1 in lifetime imaging.

The fast FLIM setup can acquire fluorescence lifetime images at frame rates of up to 840 Hz. However, in practice the frame rate is limited by the amount of fluorescence signal emitted by the specimen. The highest usable frame rate in the experiments on the OGB1 stained myocytes is 100 Hz. Here, the maximum laser power at the specimen amounts to only about 60 nW per pixel. This is well below the saturation power of the dye. Therefore, much higher frame rates are in principle possible by increasing the laser power at the specimen.

The dimensions of the fluorescence lifetime images are about  $60 \times 120$  pixels (corresponding to  $31 \times 62$   $\mu\text{m}^2$  for a  $40 \times$  objective). These comparatively small dimensions are limited by the size of the CCD chip ( $128 \times 126$  pixels) and can be increased by employing a (fast) CCD camera with larger chip size. Increasing the chip size, however, requires higher laser powers to realize the same frame rate. A chip with dimensions of  $512 \times 512$  pixels would require, for instance, 8 mW of excitation power at the specimen to realize the same frame rate.

In Fig. 6(a), a series of five images of a myocyte is shown. The upper row shows fluorescence intensity images, the middle row fluorescence lifetime images, and the lower row free calcium concentration images. The images are part of a 1000-frame-long sequence recorded at a 100-Hz frame rate. In Fig. 6(a), images are shown that are acquired 1.97, 2.02, 2.06, 2.16, and 2.60 seconds after the start of the measurement. These times correspond with the situations where the cell is in rest, the fluorescence intensity reaches about a quarter of its peak value, the fluorescence intensity reaches about half of its maximum value, the peak of the fluorescence intensity is reached, and when the rest situation is reached again respectively.

The fluorescence lifetime images are much more homogeneous than the intensity images. While the fluorescence intensity of the OGB1 stained cells is clearly higher in the center of the cell, the fluorescence lifetime images are reasonably homogeneous over the complete cell. The heterogeneity in the fluorescence intensity is due to variations in the thickness of the cell and to an inhomogeneous distribution of the OGB1 over the cell.

The FLIM-based measurements have a somewhat lower dynamic Ca range compared with the intensity measurements. This is expected from the characterization of OGB1. Furthermore, OGB1 saturates at about 500 nM. Consequently, the peak  $[\text{Ca}]_{\text{free}}$  values of 1.5  $\mu\text{M}$  cannot be quantified.

In Fig. 6(b), the fluorescence intensity and the fluorescence lifetime averaged over the whole cell are shown for a 1-sec time period that includes the time points of the images in Fig. 6(b).

The average contraction frequency of 14 myocytes amounts to about  $1.1 \pm 0.2$  Hz, one cell contracted with a frequency of 0.4 Hz and two cells contracted with a frequency of about 2 Hz. In Fig. 7, 10-sec time traces of the average fluorescence intensity and the average fluorescence lifetime of whole cells are shown for three different cells. The cells con-

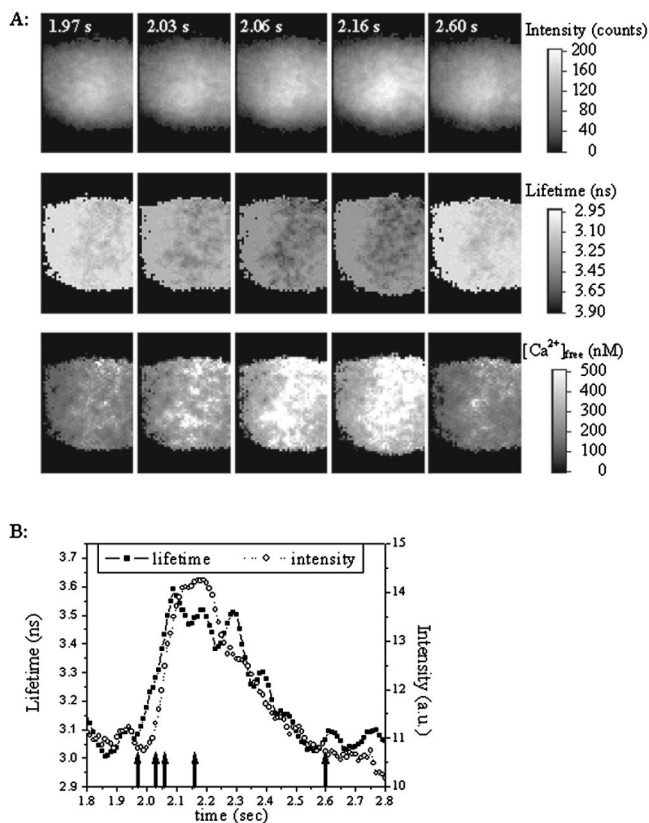


**Fig. 6** Images recorded at a 100-Hz frame rate of a neonatal rat myocyte stained with Oregon Green Bapta-1. (a) Upper row: fluorescence intensity images; middle row: fluorescence lifetime images; lower row: free calcium concentration images calculated from the lifetime images. (b) Fluorescence lifetime and intensity as a function of time, averaged over the whole myocyte.

tract with different frequencies and also the spatial distribution of the calcium fluxes of the cells differ.

Figure 7 clearly demonstrates that the fluorescence lifetime based images are not sensitive to fading due to photobleaching. While the average fluorescence intensity traces drop by  $13 \pm 4\%$  in about 10 sec due to photobleaching, the baseline of

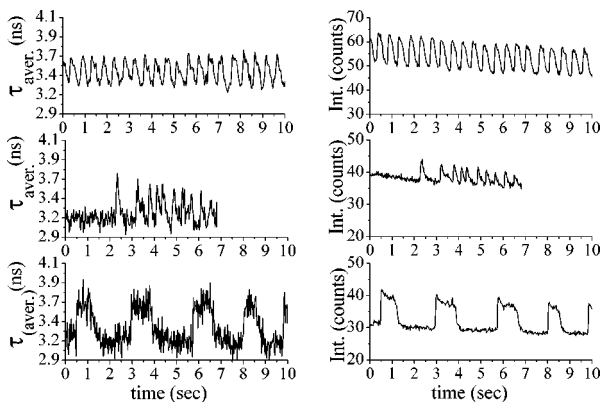


**Fig. 7** Time behavior of fluorescence lifetimes (a) and fluorescence intensities (b) of three different beating myocytes. Values are averaged over whole myocytes.

the fluorescence lifetime traces is not affected by the photobleaching and remains at the same level.

The average relative change of the fluorescence intensity amplitudes due to the beating of the myocytes amounts to  $23 \pm 8\%$  (total number of measured cells is 14). The relative change of the fluorescence lifetime is  $18 \pm 4\%$ .

The fluorescence lifetimes can be converted into calcium concentrations. The average rest value of the fluorescence lifetime amounts to  $3.2 \pm 0.1$  ns (ratio  $0.57 \pm 0.03$ ). This corresponds to about  $65 \pm 15$  nM of free calcium based on the calibration from Fig. 4. This calcium concentration is comparable with the rest calcium concentrations published for adult rat myocytes.<sup>20,21,23,25</sup> The peak calcium level, however, cannot be determined due to saturation of the fluorescent probe at  $\sim 500$  nM ( $R = 0.42$ ,  $\tau_{aver} = 3.7$  ns).

## 4 Conclusions

Here, the potential of fast fluorescence lifetime imaging is investigated. We found that the fast FLIM setup can record fluorescence lifetime images of Oregon Green Bapta-1 stained myocytes at a detection rate of up to 100 Hz. To the best of our knowledge, such high FLIM frame rates have never been achieved before. The present limit of the detection rate is due to excitation power limitations and an increase of laser power should enable even higher frame rates.

Oregon Green Bapta dyes are suitable for fast fluorescence lifetime imaging of calcium. There is not much difference between the Oregon Green Bapta-1 and Oregon Green Bapta-2 dyes for use in lifetime imaging. Both dyes can be used for fluorescence lifetime imaging of calcium concentrations in the range 1 to 500 nM. The Oregon Green Bapta-5N dye can be used for fluorescence lifetime imaging of calcium at higher concentrations of up to several  $\mu$ M. However, the fluorescence intensity of this dye is low in this calcium range.

Oregon Green Bapta-488 dyes are known to be very photo unstable.<sup>26</sup> In our measurements the fluorescence intensity of the dye drops by 13% in 10 sec at a moderate laser power level ( $30 \text{ W/cm}^2$ ). Nevertheless, photobleaching effects do not affect the fluorescence lifetime images of Oregon Green Bapta-1.

The rest calcium concentration of the neonatal rat myocytes is estimated to be about 65 nM. The dye calibration procedure on the series of buffers with varying calcium concentration may yield different values from a calibration in cells; however, there are several indications that the calibration is reasonable. First of all the rest value of the free Ca concentration is within the range of values reported in literature (50 to 200 nM). Second, earlier work on the calibration of fluorescence lifetime based ion concentration sensing revealed that calibrations in buffer compare well with calibrations carried out in cells.<sup>9,10</sup> Whether this is also the case for the Oregon Green Bapta dyes needs to be confirmed.

## Acknowledgments

We would like to thank E. Klarenbeek for his assistance during the building of the setup, R. Steenbergen for the preparation of the neonatal myocytes, and W.G.J.H.M. van Sark for his valuable comments. This research is supported by the EC

Frame work V program, project number QL3-CT-1999-01340 and the Dutch Technology Foundation (STW), project number UNS 3946.

### References

1. T. Takamatsu and W. G. Wier, "High temporal resolution video imaging of intracellular calcium," *Cell Calcium* **11**, 111–120 (1990).
2. B. Gabriel and J. Teissié, "Fluorescence imaging in the millisecond time range of membrane electroporation of single cells using a rapid ultra-low-light intensifying detection system," *Eur. Biophys. J.* **27**, 291–298 (1998).
3. G. Grynkiewicz, M. Poenie, and R. Y. Tsien, "A new generation of  $\text{Ca}^{2+}$  indicators with greatly improved fluorescence properties," *J. Biol. Chem.* **260**, 3440–3450 (1985).
4. R. Y. Tsien and M. Poenie, "Fluorescence ratio imaging: a new window into intracellular ionic signaling," *Trends Biochem. Sci.* **11**, 450–455 (1986).
5. T. J. Rink, R. Y. Tsien, and T. Pozzan, "Cytoplasmic pH and free  $\text{Mg}^{2+}$  in lymphocytes," *J. Cell Biol.* **95**, 189–196 (1982).
6. M. Maravall, Z. F. Mainen, B. L. Sabatini, and K. Svoboda, "Estimating intracellular calcium concentrations and buffering without wavelength ratioing," *Biophys. J.* **78**, 2655–2667 (2000).
7. J. R. Lakowicz, H. Szmajda, K. Nowaczyk, and M. L. Johnson, "Fluorescence lifetime imaging of calcium using Quin-2," *Cell Calcium* **13**, 131–147 (1992).
8. J. R. Lakowicz, in *Principles of Fluorescence Spectroscopy*, Plenum Publishers, New York (1999).
9. R. Sanders, H. C. Gerritsen, A. Draaijer, P. M. Houpt, and Y. K. Levine, "Quantitative pH imaging in cells using confocal fluorescence lifetime imaging microscopy," *Anal. Biochem.* **22**, 302–310 (1995).
10. B. Herman, P. Wodnicki, S. Kwon, A. Periasamy, G. W. Gordon, N. Mahajan, and X. F. Wang, "Recent developments in monitoring calcium and protein interactions in cells using fluorescence lifetime microscopy," *J. Fluoresc.* **7**, 85–91 (1997).
11. J. Mizeret, T. Stepinac, M. Hansroul, A. Studzinski, H. van den Bergh, and G. Wagnières, "Instrumentation for real-time fluorescence lifetime imaging in endoscopy," *Rev. Sci. Instrum.* **70**, 4689–4701 (1999).
12. O. Holub, M. J. Seufferheld, C. Gohlke, Govindjee, and R. M. Clegg, "Fluorescence lifetime imaging (FLI) in real-time—a new technique in photosynthesis research," *Photosynthetica* **38**, 581–599 (2000).
13. E. P. Buurman, R. Sanders, A. Draaijer, H. C. Gerritsen, J. J. Van Veen, P. M. Houpt, and Y. K. Levine, "Fluorescence lifetime imaging using a confocal laser scanning microscope," *Scanning* **14**, 155–159 (1992).
14. J. Sytsma, J. M. Vroom, C. J. de Grauw, and H. C. Gerritsen, "Time gated fluorescence lifetime imaging and micro-volume spectroscopy using two photon excitation," *J. Microsc.* **191**, 39–51 (1998).
15. A. D. Scully, R. B. Ostler, D. Phillips, P. O'Neill, K. M. S. Townsend, A. W. Parker, and A. J. MacRobert, "Application of fluorescence lifetime imaging microscopy to the investigation of intracellular PDT mechanisms," *Bioimaging* **5**, 9–18 (1997).
16. C. J. de Grauw and H. C. Gerritsen, "Multiple time-gate module for fluorescence lifetime imaging," *Appl. Spectrosc.* **55**, 670–678 (2001).
17. A. V. Agronskaia, L. G. J. Tertoolen, and H. C. Gerritsen, "High frame rate fluorescence lifetime imaging," *J. Phys. D* **36**, 1655–1662 (2003).
18. C. J. de Grauw, J. M. Vroom, H. T. M. der Voort, and H. C. Gerritsen, "Imaging properties in two-photon excitation microscopy and effects of refractive-index mismatch in thick specimens," *Appl. Opt.* **38**, 5995–6003 (1999).
19. R. Sanders, H. C. Gerritsen, A. Draaijer, P. M. Houpt, and Y. K. Levine, "Fluorescence lifetime imaging of free calcium in single cells," *Bioimaging* **2**, 131–138 (1994).
20. M. S. Jafri, J. J. Rice, and R. L. Winslow, "Cardiac  $\text{Ca}^{2+}$  dynamics: the roles of ryanodine receptor adaptation and sarcoplasmic reticulum load," *Biophys. J.* **74**, 1149–1168 (1998).
21. M. B. Cannell, H. Cheng, and W. J. Lederer, "Spatial non-uniformities in  $[\text{Ca}^{2+}]_i$  during excitation-contraction coupling in cardiac myocytes," *Biophys. J.* **67**, 1942–1956 (1994).
22. J. R. Berlin and M. Konishi, " $\text{Ca}^{2+}$  transients in cardiac myocytes measured with high and low affinity  $\text{Ca}^{2+}$  indicators," *Biophys. J.* **65**, 1632–1647 (1993).
23. D. W. Piston, M. S. Kirby, H. Cheng, W. J. Lederer, and W. W. Webb, "Two-photon-excitation fluorescence imaging of three-dimensional calcium-ion activity," *Appl. Opt.* **33**, 662–669 (1994).
24. M. Canepari and F. Mammano, "Imaging neuronal calcium fluorescence at high spatio-temporal resolution," *J. Neurosci. Methods* **87**, 1–11 (1999).
25. J. R. Berlin, J. W. M. Bassani, and D. M. Bers, "Intrinsic cytosolic calcium buffering properties of single rat cardiac myocytes," *Biophys. J.* **67**, 1775–1787 (1994).
26. D. Thomas, S. C. Tovey, T. J. Collins, M. D. Bootman, M. J. Berridge, and P. Lipp, "A comparison of fluorescent  $\text{Ca}^{2+}$ -indicator properties and their use in measuring elementary and global  $\text{Ca}^{2+}$  signals," *Cell Calcium* **28**, 213–223 (2000).